

8

MAGNETIC RESONANCE EXPERIMENTS

1. Introduction

As we know† when a quantum-mechanical system, for example, an atom (or a nucleus), with angular momentum L , (or I), different from zero, is placed in a magnetic field H , the energy states having different values for the quantum number m acquire an additional energy

$$\Delta E = \frac{\mu}{I} Hm \quad (1.1)$$

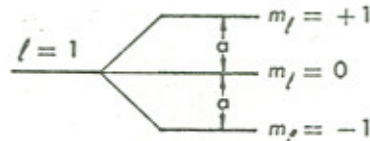
where μ is the "magnetic moment" of the system. For systems involving electrons, μ is of the order of the Bohr magneton μ_0 , while for nuclei μ is of the order of the nuclear magneton, μ_N . In convenient units

$$\begin{aligned} \mu_0/h &= & 1.401 \text{ Mc/gauss} \\ \mu_N/h &= (\mu_0/h)/1836 = 0.762 \text{ kc/gauss} \end{aligned} \quad (1.2)$$

† This subject was discussed in detail in Chapter 7; see especially Section 2.

In Fig. 8.1 is shown the splitting of an energy state with $l = 1$ into its three sublevels. As noted in Chapter 7, in atomic systems we do not observe the spontaneous transitions (labeled a in the figure) between sublevels with different m_l , because they do not satisfy the selection rule $\Delta l = \pm 1$. Instead the splitting of a level is observed through the small change in the frequency of the radiation emitted in the transitions between widely distant levels (with $\Delta l = \pm 1$). It is clear that if we could directly measure the frequency corresponding to a transition between the m_l sublevels of the same state, a much more precise knowledge of the energy splitting would be obtained.

FIG. 8.1 Splitting of an energy level with $l = 1$ into three components when placed in a magnetic field.



Now, the selection rule $\Delta l = \pm 1$ is applicable to electric dipole radiation; however, transitions with $\Delta l = 0 \Delta m = \pm 1$ do occur when *magnetic dipole* radiation is emitted, but the probability for such a transition is reduced by a factor† $(v/c)^2$ from the case of an electric dipole transition. We therefore conclude that spontaneous transitions with $\Delta l = 0 \Delta m = \pm 1$ will be very rare, especially if the system can return to its ground state (lowest energy state) by a $\Delta l = \pm 1$ transition. On the other hand, in the presence of an electromagnetic field, *induced* transitions have a probability of occurring if the frequency of the field is equal (or at least fairly close) to the energy difference between the two levels; induced transitions towards higher or lower energy states are equally probable. Further, the transition probability is proportional to the square of the strength of the electromagnetic field (that is, the total number of quanta) so that if a sufficiently strong radiofrequency (rf) magnetic field (of frequency ν_0) is available, magnetic dipole transitions should take place.

By referring to Eq. 1.2, we note that for a field of a few kilogauss the energy splitting corresponds, for nuclei, to a frequency of megacycles, and for electrons, to a few kilomegacycles, that is, to frequencies that can be easily generated in the laboratory. A calculation also shows that a radio-frequency magnetic field of a fraction of a gauss is more than sufficient, in most cases, to cause transitions. A field intensity of 1 oersted corresponds to

$$\tilde{S} = \frac{1}{2} \sqrt{\frac{\mu_0}{\epsilon_0}} H^2 = \frac{1}{2} \sqrt{\frac{4 \times 10^{-7}}{8.85 \times 10^{-12}}} \times \left(\frac{10^3}{4\pi}\right)^2 \text{ (MKS)} \approx 2.35 \times 10^2 \frac{\text{watts}}{\text{cm}^2} \quad (1.3)$$

† For atomic systems v is of the order of the velocity in a Bohr orbit, namely, $v/c \approx 5 \times 10^{-6}$.

so that radiofrequency fields of adequate intensity can be generated. Finally, we must be able to detect the fact that a transition took place; this may be done in several ways and is one of the major distinctions between the various types of magnetic resonance experiments.

For example, in the first magnetic resonance experiment, performed by I. Rabi and collaborators in 1939, a beam of atoms having $J = \frac{1}{2}$ was passed in succession through two very inhomogeneous magnets A and B shown in Fig. 8.2. A homogeneous magnetic field existed in the intermediate region C . If a transition took place in region C from a state $m = +\frac{1}{2}$ to $m = -\frac{1}{2}$, that particular atom was deflected in an opposite direction in field B and thus missed the detector. Hence, resonance was detected by a decrease in beam current when the frequency of the radiofrequency was the appropriate one for the magnetic field strength in C .

Another method for detecting the occurrence of resonance is to observe the absorption of energy from the radiofrequency field when transitions toward higher energy levels take place. This is the technique used in most nuclear magnetic resonance (nmr) experiments and in electron magnetic resonance (called "electron paramagnetic resonance," epr) experiments; these will be described in some detail in Sections 4 and 5. In experiments with atomic vapors or transparent materials it is possible to detect the magnetic resonance effect by changes in the polarization of the atomic radiation ($\Delta m \neq 0$) or by selective absorption effects; such an experiment is described in Section 6.

Apart from its intrinsic interest as a way of inducing transitions between the energy sublevels of a quantum-mechanical system (atom, nucleus), magnetic resonance has become an important tool of physics. The atomic beam experiments of Rabi and his coworkers mentioned before led to very precise measurements of the hyperfine structure of atomic systems and thus to accurate values of the nuclear moments. The measurement of the "Lamb shift" (between the $2S_{1/2}$ and $2P_{1/2}$ levels of hydrogen) is an example of such a measurement, as is the very precise determination of the anom-

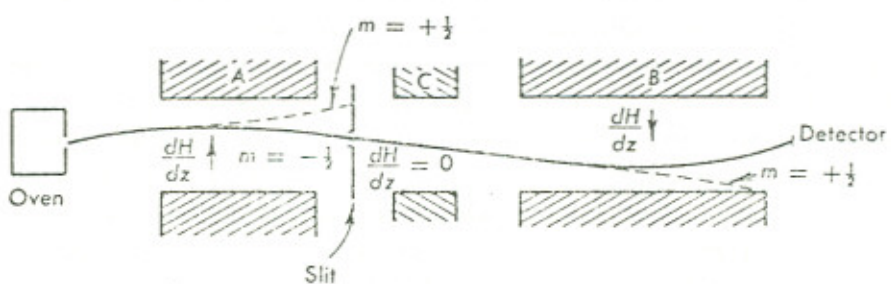


FIG. 8.2 The atomic beam arrangement of I. Rabi and collaborators used to detect magnetic resonance transitions in atomic energy levels.

alous magnetic moment of the electron. (The g factor of the electron is not $g = 2.00$ as stated in Chapter 7 but $g = 2.00232$ (!) as predicted by quantum electrodynamics).

A nuclear magnetic resonance experiment consists in inducing transitions between the sublevels of a nucleus placed in an external magnetic field (in the terminology of Chapter 7, we would call it the Zeeman effect of the nucleus). However, the atom to which the nucleus belongs must have $J = 0$ (diamagnetic material), since otherwise the nuclear spin would be coupled to J and the large electronic magnetic moment would mask the effect. By means of such experiments, nuclear magnetic moments are measured directly and to a high accuracy.

As will be explained in Section 3, the observation of nuclear magnetic resonance in solids and liquids† depends on the relaxation of the nuclear spins through their interaction with the lattice. Thus nuclear magnetic resonance studies have yielded a very large amount of information on the solid-state properties of many materials.

Soon after the first successful nuclear magnetic resonance experiments, it was realized that the width of the observed resonance line for protons was mostly due to inhomogeneities in the constant magnetic field that is used to split the energy sublevels. When a very homogeneous field was applied, the proton resonance line was shown to exhibit a fine structure of the order of 0.01 gauss. This structure depends on the organic compound to which the hydrogens of the sample belong. With even more homogeneous fields a hyperfine structure of the order of 0.001 gauss, is observed. Thus today nuclear magnetic resonance has become a very important tool of analytical chemistry as well.

We speak of paramagnetic resonance when the magnetic moments of electrons are involved in the transitions. This occurs in the study of molecular spectra (where, however, electric dipole transitions are also induced); this field being known as "microwave spectroscopy." Indeed the separation of many molecular energy levels falls conveniently in the microwave bands (millimeter and submillimeter wavelengths), and by using gaseous samples very narrow lines can be obtained.

However, the term paramagnetic resonance is mainly used for transitions between the Zeeman levels of quasi-free electrons in liquids and solids; a more adequate term also frequently used is electron spin resonance. In principle, we should always measure a g factor of 2.00 (if we deal with free electrons), which would not be interesting; instead a great variety of g factors and structure appears in the resonance lines due to the different effective coupling of the electron with the crystalline field. These effects depend on the relative orientation of the magnetic field H_0 and the crystal axis.

† Frequently referred to as *nuclear magnetic resonance* in bulk matter.

Thus electron paramagnetic resonance has become a very important tool in the study of crystalline structures as well as in the identification of free radicals in chemistry, medicine, and biophysics.

Section 2 will deal briefly with the conditions for inducing a magnetic dipole transition between two levels of a quantum-mechanical system ... we will also discuss the classical analogue to this phenomenon. In Section 3 the mechanisms which are essential for the observation of energy absorption in nuclear magnetic resonance and electron paramagnetic resonance experiments are introduced; namely relaxation and saturation. In Section 4 the techniques and results of nuclear magnetic resonance experiments on protons are presented, and in Section 5 data on electron spin resonance obtained at microwave frequencies are given. Section 6 describes an electron paramagnetic resonance experiment with optical detection of the resonance condition, the so called "double resonance" technique.

REFERENCES

As always, the discussion presented here is limited, and undoubtedly the reader will wish to refer to some of the many excellent monographs and texts written on this subject. The following are suggested:

- A. Abragam, *The Principles of Nuclear Magnetism*, Oxford University Press, 1961.
The outstanding work on nuclear magnetic resonance. The treatment is theoretical and advanced, but very complete and clear.
- E. R. Andrew, *Nuclear Magnetic Resonance*, Cambridge University Press, 1956. A short text containing experimental details as well; it is very useful to the students in this course.
- C. H. Townes and A. L. Shawlow, *Microwave Spectroscopy*, McGraw-Hill, 1955. An extensive and comprehensive work on the subject, mainly treating the molecular spectra obtained in gases.
- G. E. Pake, *Paramagnetic Resonance*, Benjamin, 1962.
- D. J. E. Ingram, *Spectroscopy at Radio and Microwave Frequency*, Butterworth, 1955.
Very helpful for the study of paramagnetic resonance in solids and crystalline materials.

2. Magnetic Dipole Transitions between the m Sublevels of a Quantum-Mechanical System

Let us consider a system (for example, a nucleus) with angular momentum I (magnitude $\hbar\sqrt{I(I+1)}$) and magnetic moment μ oriented along the spin axis. It is customary (for nuclei) to express the proportionality between the spin I and magnetic moment μ by

$$\mu = \gamma\hbar I \quad (2.1)$$

Here γ is the gyromagnetic ratio, and as can be seen from Eq. 2.3, it has dimensions of radians per sec-gauss.

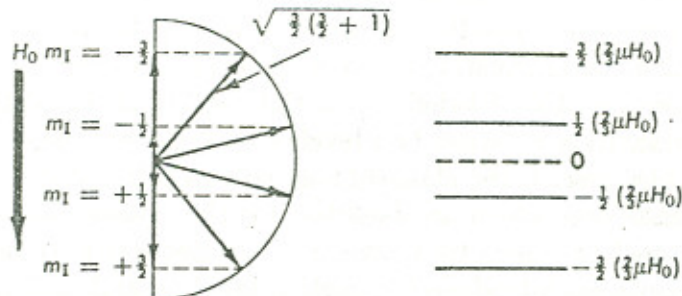


FIG. 8.3 The energy of the four sublevels of a nucleus with spin $I = \frac{1}{2}$ when placed in a magnetic field H_0 . Note that the energy depends on the "orientation" of the spin with respect to H_0 ; also the magnitude of the spin vector is $|I| = \sqrt{\frac{1}{2}(\frac{1}{2} + 1)}$.

In the presence of an external magnetic field H_0 , the nucleus can be in any of the $(2I + 1)$ sublevels labeled by m_I as shown also in Fig. 8.3. We can then write for the energy† of these sublevels (Eq. 1.1)

$$\frac{E}{\hbar} = -\gamma H_0 m \quad (2.2)$$

so that the energy difference between any adjacent sublevels ($\Delta m = \pm 1$) is simply

$$\frac{\Delta E}{\hbar} = \gamma H_0 = \omega_0 \quad (2.3)$$

Let us then further consider the simplest case, namely, $I = \frac{1}{2}$, in which only two sublevels exist, $m = -\frac{1}{2}$ and $m = +\frac{1}{2}$. In addition to H_0 , let a weak field H_1 , rotating in a plane normal to H_0 with an angular frequency ω be introduced. Taking as usual the z axis along H_0 , we write the two components of H_1 as follows:

$$(H_1)_z = H_z = H_1 \cos \omega t \quad (H_1)_y = H_y = H_1 \sin \omega t$$

and

$$H_1 \ll H_0$$

The additional energy of the nucleus, due to the field H_1 is

$$\mathfrak{H}_1 = \mathbf{g} \cdot \mathbf{H}_1 = \gamma \hbar (H_z I_z + H_y I_y) = \frac{\gamma \hbar H_1}{2} (I_+ e^{-i\omega t} + I_- e^{+i\omega t}) \quad (2.4)$$

† Instead of energy, we use for convenience angular frequency; the transition frequency is $\Delta\nu = (\Delta E/\hbar)/(2\pi) = \omega_0/2\pi$.

where†

$$I_+ = I_x + iI_y \quad \text{and} \quad I_- = I_x - iI_y \quad (2.5)$$

Since the energy specified by Eq. 2.4 is very small as compared to that given by Eq. 2.2, it can be treated as a time-dependent perturbation; thus, to first order, the transition probability is proportional to the absolute square of the matrix element

$$M = \frac{\gamma\hbar H_1}{2} \langle f | I_+ e^{-i\omega t} + I_- e^{i\omega t} | i \rangle \quad (2.6)$$

where i and f stand for the initial and final state. As usual the matrix element is evaluated by performing the integral

$$\int \psi_f^* \mathcal{H}_1 \psi_i d^3x dt \quad (2.7)$$

and we must include the time dependence of the wave functions

$$\begin{aligned} \psi_f &= u(I, m') \exp\left(-i \frac{E'}{\hbar} t\right) \\ \psi_i &= u(I, m) \exp\left(-i \frac{E}{\hbar} t\right) \end{aligned} \quad (2.8)$$

Here primes refer to the final state, and $u(I, m)$ stands for the space part of the wave function. Evaluating Eq. 2.6 with the help of Eqs. 2.7 and 2.8, we find

$$\begin{aligned} M &= \frac{\gamma\hbar H_1}{2} \left\{ \langle I, m' | I_+ | I, m \rangle \int \exp\left[-i\left(\frac{E - E'}{\hbar} + \omega\right)t\right] dt \right. \\ &\quad \left. + \langle I, m' | I_- | I, m \rangle \int \exp\left[-i\left(\frac{E - E'}{\hbar} - \omega\right)t\right] dt \right\} \quad (2.9) \end{aligned}$$

The matrix elements of the operators I_+ and I_- are§

$$\begin{aligned} \langle m' | I_+ | m \rangle &= \sqrt{I(I+1) - m(m+1)} \delta_{m', m+1} \\ \langle m' | I_- | m \rangle &= \sqrt{I(I+1) - m(m-1)} \delta_{m', m-1} \end{aligned} \quad (2.9a)$$

† We expand the exponentials and obtain

$(I_x \cos \omega t + iI_y (-i) \sin \omega t) + (I_x \cos \omega t - iI_y (+i) \sin \omega t)$
 $= 2(I_x \cos \omega t + I_y \sin \omega t).$

‡ See, for example, E. Fermi, *Notes on Quantum Mechanics*, University of Chicago Press, lecture 23.

§ See E. Fermi, *Notes on Quantum Mechanics*, loc. cit. Lecture 28.

and thus I_+ connects only states with $m' - m = 1$ while I_- connects states $m' - m = -1$. For $I = \frac{1}{2}$ the above matrix elements reduce to 1 for either I_+ or I_- . The integrals over the time are essentially δ functions (but see below) expressing the conservation of energy and showing that the transition probability is different from zero only if

$$\begin{aligned} E' - E &= \hbar\omega \quad \text{for} \quad m' = m + 1 \\ \text{and} \quad E - E' &= \hbar\omega \quad \text{for} \quad m' = m - 1 \end{aligned} \quad (2.10)$$

that is, when the angular frequency of the rotating field is equal to the energy difference between adjacent m sublevels. Using Eq. 2.3, the condition of Eqs. 2.10 becomes

$$\hbar\omega = \hbar\gamma H_0 = \hbar\omega_0 \quad (2.10a)$$

Indeed, the integrals in Eq. 2.9 would represent δ functions if the integration was from $t = 0$ to $t = \infty$. We know, however, from the treatment of time-dependent perturbation theory† that the integrals are to be taken from $t = 0$ to $t = t$, the time of observation. If we start from an initial state i and integrate over a continuum of final states f , we obtain for the transition rate (transition probability *per unit time*)

$$R_{if} = \frac{2\pi}{\hbar} |\mathfrak{M}|^2 \rho(E) \quad (2.11)$$

Here \mathfrak{M} is the time independent part of the matrix element given by Eq. 2.9 (that is, without the integrals). $\rho(E)$ is the "density of final states" and gives the number of states f per unit energy interval that have energy close to E' . For example, if the final state f has an extremely well-defined energy E_0 , then $\rho(E) \rightarrow \delta(E - E_0)$; if the final state has a certain width (due for example to a finite lifetime‡ or other broadening effects), then $\rho(E)$ expresses this fact mathematically. We require the function $\rho(E)$ to be normalized and can also express it in terms of frequency

$$\rho(E) = \rho(h\nu) = \frac{1}{h} g(\nu)$$

with

$$\int \rho(E) dE = \int g(\nu) d\nu = 1 \quad (2.12)$$

Combining Eqs. 2.9, 2.11, and 2.12 we finally obtain for the transition rate in the case $I = \frac{1}{2}$

$$R_{-1/2 \leftrightarrow +1/2} = R_{+1/2 \leftrightarrow -1/2} = \frac{\gamma^2 H_1^2}{4} g(\nu) \quad (2.13)$$

† See E. Fermi, *Notes*, or L. Schiff, *Quantum Mechanics*, McGraw-Hill, Chapter VII.

‡ Cf. Chapter 6, Section 4 on the Mössbauer effect.

where ν is the frequency of the radiofrequency and $g(\nu)$ gives the shape of the resonance line; clearly $g(\nu)$ will be significantly different from zero only for $\nu \approx \nu_0$.

At this point it is important to note from Eq. 2.9 that the probability that the rotating field H_1 will induce a transition from $m_1 \rightarrow m_2$ (where $m_1 - m_2 = +1$) is always the same as for inducing the transition $m_2 \rightarrow m_1$. Therefore, for the case $I = \frac{1}{2}$ we see that the effect of the radiofrequency field is to *equalize the population* of the two states.[†]

The reader should keep in mind that Eq. 2.13 was obtained from a perturbation calculation; however, the exact value for the transition probability for $I = \frac{1}{2}$ or for any arbitrary spin can also be calculated.

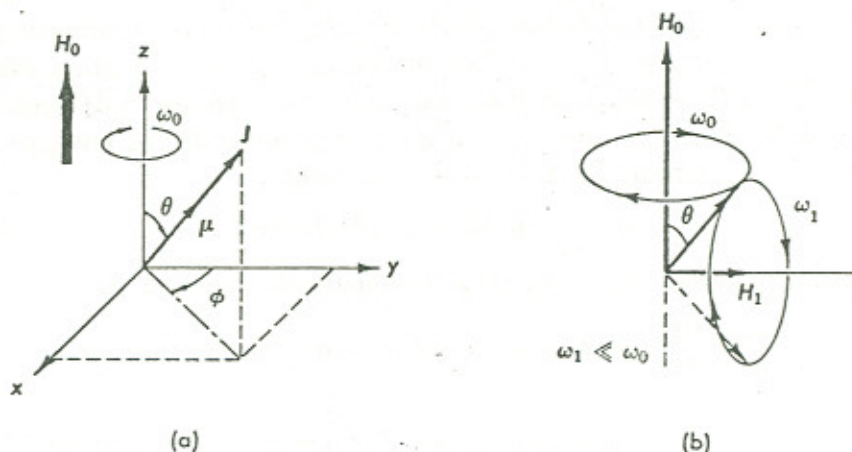


FIG. 8.4 Precession of a magnetic moment μ when placed in a magnetic field H_0 . (a) The spin precesses with angular frequency $\omega_0 = \gamma H_0$; the angle θ is a constant of the motion. (b) In addition to H_0 a weak magnetic field H_1 is now also applied. H_1 is rotating about the z axis with angular frequency ω_1 , and therefore μ precesses about H_1 with angular frequency $\omega_1 = \gamma H_1$; θ is not any more conserved.

Finally, we will briefly show how the effect of a rotating radiofrequency field can be understood also on the basis of a classical model. Consider again a nucleus with spin I and magnetic moment $\mu = \gamma \hbar I$. Let J be the magnitude of the angular momentum, which classically[‡] will be just $J = \hbar I$, and let it make an angle θ with the z axis as shown in Fig. 8.4a. If a constant magnetic field H_0 is applied along the z axis, it will exert a torque on the magnetic moment, given by

$$\tau = \mu \times H_0 = \gamma(J \times H_0) \quad (2.14)$$

[†]This argument can be generalized to $I > \frac{1}{2}$ as well.

[‡]As we recall the magnitude of any angular momentum vector I , is given quantum mechanically by $\hbar\sqrt{I(I+1)}$.

This must equal the time derivative of the angular momentum.

$$\frac{d\mathbf{J}}{dt} = \boldsymbol{\tau} = \gamma(\mathbf{J} \times \mathbf{H}_0) \quad (2.15)$$

As we know from the theory of the gyroscope, the solution† of Eq. 2.15 leads to a precession of the angular momentum vector \mathbf{J} about the z axis, preserving the angle θ , and at an angular frequency ω_0 independent of θ ,

$$\omega_0 = -\frac{|d\mathbf{J}/dt|}{|\mathbf{J} \times \mathbf{n}_z|} \mathbf{n}_z = -\gamma H_0 \mathbf{n}_z \quad (2.16)$$

where \mathbf{n}_z is the unit vector in the z direction.

This phenomenon is called the Larmor precession and the angular frequency given by Eq. 2.16 is the "Larmor" frequency. It is fascinating even though not surprising that the Larmor frequency has the same value as given by Eq. 2.3 for the transition frequency between any adjacent levels ($\Delta m = \pm 1$). Further, since the angle θ is preserved, the energy of the nucleus in the magnetic field remains a constant

$$E = -\mathbf{p} \cdot \mathbf{H} = -\gamma \hbar I H_0 \cos \theta \quad (2.17)$$

† By referring to Fig. 8.4a, we write for the equation of motion (2.15)

$$\frac{dJ_z}{dt} = \frac{d}{dt} (J \sin \theta \sin \phi) = \gamma [J_y H_z - 0] = \gamma J \sin \theta \cos \phi H_0$$

$$\frac{dJ_y}{dt} = \frac{d}{dt} (J \sin \theta \cos \phi) = \gamma [0 - J_z H_z] = -\gamma J \sin \theta \sin \phi H_0$$

$$\frac{dJ_x}{dt} = \frac{d}{dt} (J \cos \theta) = \gamma [0 - 0] = 0$$

J does not change in magnitude because

$$\frac{d}{dt} (J^2) = \frac{d}{dt} (\mathbf{J} \cdot \mathbf{J}) = 2\mathbf{J} \cdot \frac{d\mathbf{J}}{dt} = 2\mathbf{J} \cdot (\mathbf{J} \times \mathbf{H}_0)\gamma = 0$$

but $\mathbf{J} \times \mathbf{H}_0$ is normal to \mathbf{J} so that the above expression is zero. Given then this fact we note from the third equation that $d \cos \theta/dt = 0$; that is, θ is constant of the motion. For the first two equations we write

$$\frac{d}{dt} \sin \phi = \cos \phi \frac{d\phi}{dt} = \gamma H_0 \cos \phi$$

$$\frac{d}{dt} \cos \phi = -\sin \phi \frac{d\phi}{dt} = -\gamma H_0 \sin \phi$$

that is,

$$\frac{d\phi}{dt} = \omega_0 = \gamma H_0$$

We now introduce an additional weak magnetic field H_1 oriented in the $x - y$ plane and rotating about the z axis (in the same direction as the "Larmor precessing" spin \mathbf{I}) with an angular frequency ω . If the frequency ω is different from ω_0 , the angle between the field H_1 and the magnet moment \mathbf{u} will continuously change so that their interaction will average out to zero. If, however, $\omega \approx \omega_0$, the angle between \mathbf{u} and H_1 is maintained and a net interaction is effective (Fig. 8.4b). If we look at the system in a reference frame that is rotating about the z axis with the angular velocity ω_0 , then the spin will appear to make an angle $\psi = 90^\circ - \theta$ with H_1 , and according to the previous argument will start to precess (in the rotating frame) about H_1 . This corresponds to a "nutation" and a consequent change of the angle θ , which implies a change in the potential energy of the nucleus in the magnetic field (Eq. 2.17). The change in θ is the classical analogy to a *transition* between sublevels with different m . We see that (a) such transitions may take place only if the rotating field has an angular frequency $\omega = \omega_0 = \gamma H_0$, and (b) since the angle θ will continuously change (with an angular frequency $\omega_1 = \gamma H_1$). The effect of the radiofrequency is to populate, on the average, all values of θ , that is *all levels, equally*.

3. Absorption of Energy by the Nuclear Moments.

3.1 RELAXATION AND SATURATION

We saw in Section 2 that a radiofrequency magnetic field may indeed induce transitions between the m sublevels of a quantum-mechanical system. In the case of atomic-beam or optical double resonance experiments the atoms are essentially free, while in nuclear magnetic resonance (and electron paramagnetic resonance) experiments the nuclei (electrons) are in constant interaction with their surroundings. There are mainly two types of interactions,[†] (a) *spin-lattice*, in which the nuclear spin interacts with the entire solid or liquid, transferring energy from the spin system to the lattice; and (b) *spin-spin*, in which the nuclear spin interacts with a neighboring nuclear spin, but the total energy of the spin system remains constant. As a matter of fact, it is the spin-lattice interaction that makes possible the observation of energy absorption from the radiofrequency field when the resonance frequency is reached.

To understand this last statement, consider again the simple case of a nucleus with spin $I = \frac{1}{2}$. In the presence of a magnetic field H_0 it is split into the two energy sublevels with $m = +\frac{1}{2}$ and $m = -\frac{1}{2}$. As remarked before, the rate (Eq. 2.11) for transitions

$$(m = +\frac{1}{2}) \rightarrow (m = -\frac{1}{2}) \quad (3.1)$$

[†] We will not consider quadrupole interactions or other relaxation mechanisms.

is equal to the rate for transitions

$$(m = -\frac{1}{2}) \rightarrow (m = +\frac{1}{2}) \quad (3.2)$$

The number of transitions per unit time is given in either case by

$$R_{if} \times N_i \quad (3.3)$$

where N_i is the number of nuclei in the initial state. Further, transitions of the type in Eq. 3.1 absorb energy from the radiofrequency field while transitions of the type in Eq. 3.2 give energy to the radiofrequency field.† Thus the net power absorbed from the radiofrequency field is as given in Eq. 3.4. (We also multiply by the energy necessary for one transition.)

$$P = [N_{+1/2} \times R(+\frac{1}{2} \rightarrow -\frac{1}{2})] \hbar \omega_0 - [N_{-1/2} \times R(-\frac{1}{2} \rightarrow +\frac{1}{2})] \hbar \omega_0 = (N_{+1/2} - N_{-1/2}) R \hbar \omega_0 \quad (3.4)$$

Thus if $N_{-1/2} = N_{+1/2}$, no net power can be absorbed from the field. However, if we consider a system consisting of a large number of spins in equilibrium with its surroundings, it is known from a very general theorem of statistical mechanics that every state of energy E will be populated according to the Boltzmann distribution

$$N(E) = N_0 e^{-E/kT} \quad (3.5)$$

with k the Boltzmann constant and T the absolute temperature in degrees K. It follows that for a system of N spins I in the presence of a magnetic field H_0 , each m sublevel will be populated according to

$$N(m) = \frac{N}{2I + 1} \exp\left(+\frac{m\gamma\hbar H_0}{kT}\right) \quad (3.6)$$

The normalizing factor was approximated by $N/(2I + 1)$, which holds‡ for $\gamma\hbar H_0 \ll kT$; $-m\gamma\hbar H_0$ is the energy of the m sublevel (see Eq. 2.2). Note that T in Eq. 3.6 is the temperature of the spin system and equals the lattice temperature, if no external perturbations (such as the radiofrequency field) are present.

It follows from Eq. 3.6 that the populations $N_{+1/2}$ and $N_{-1/2}$ entering Eq. 3.4 in our previous discussion ($I = \frac{1}{2}$) will not be equal. Indeed, there will be a number of excess nuclei N_s , in the lower energy state given by

$$N_s = N_{+1/2} - N_{-1/2} = \frac{N}{2} \left[\exp\left(+\frac{\hbar\omega_0}{2kT}\right) - \exp\left(-\frac{\hbar\omega_0}{2kT}\right) \right] \quad (3.7)$$

† Remember Eq. 22.

‡ Indeed, if we expand the exponential through first order, we obtain correctly

$$\sum_{m=-I}^{m=I} N(m) = N$$

and since $\omega_0\hbar$ is always much smaller than kT_s , we may write Eq. 3.7 as

$$N_s \approx \frac{N}{2} \frac{\hbar\omega_0}{kT} \quad (3.7a)$$

It is only these N_s nuclei that can contribute towards a net absorption of energy, and the power (Eq. 3.4) is given by

$$P = N_s \times R \times \hbar\omega_0 = \frac{N}{2} \frac{\hbar\omega_0}{kT} \times (\hbar\omega_0) \times R \quad (3.8)$$

Before proceeding further, we calculate some numerical values: for protons $\gamma = 2.673 \times 10^4$ rad/sec-gauss, so that for $H_0 = 10^4$ gauss and $T = 300^\circ K$ we obtain

$$\frac{N_s}{N} = \frac{\omega_0\hbar}{2kT} = \frac{(2.67 \times 10^8) \times (6.6 \times 10^{-16}) \text{ eV}}{2(1/40) \text{ eV}} \approx 4 \times 10^{-6}$$

which justifies the approximation used in going from Eq. 3.7 to Eq. 3.7a. If we further consider a sample of 1 cm^3 of water, the number of protons contained in it is

$$N = N_0 \times (2/18) = 6 \times 10^{23} \times (2/18) = (2/3) \times 10^{23}$$

If we use for $R = 1/\text{sec}$ (as can be seen from Eq. 2.13, this is a conservative value; R , however, can be as large as $10^3/\text{sec}$ as discussed below), we obtain for Eq. 3.8

$$P = (\hbar\omega_0) \times \left(N \times \frac{\hbar\omega_0}{2kT_s} \right) \times R \approx 5 \times 10^{10} \text{ eV/sec} = 8 \times 10^{-9} \text{ watts} \quad (3.9)$$

This is a very small amount of power, especially since the applied radio-frequency field may be of the order of milliwatts. Therefore, a sensitive null method greatly facilitates the observation of nuclear resonance absorption.

Now in writing down Eq. 3.8, we assume that the power absorbed is proportional to the number of excess nuclei n_s ; but as transitions are induced to the upper state, the number n_s will continuously decrease. The decrease will be exponential at a rate R

$$n_s = N_s e^{-Rt} \quad (3.10)$$

Soon the populations of the two levels will be equalized, $N_{+1/2} = N_{-1/2}$ and no more absorption will be observed.

However, while the radiofrequency field tends to equalize the populations, the "spin-lattice" interaction tends to restore the Boltzmann dis-

tribution as given by Eqs. 3.7 and 3.7a at a rate characterized by $1/T_1$. We say that the nuclei are "relaxed" through their interaction with the lattice, and the characteristic time T_1 for this process is called the *spin-lattice relaxation time*. Therefore, in the presence of a radiofrequency field tuned to the resonance frequency, the number of excess nuclei at equilibrium n_s , depends on T_1 and on R ; if $R \ll 1/T_1$, then $n_s \rightarrow N_s$, while if $R \gg 1/T_1$, $n_s \rightarrow 0$. The value of n_s can be easily obtained†

$$n_s = \frac{N_s}{1 + 2RT_1} \quad (3.11)$$

where N_s as given by Eqs. 3.7 and 3.7a is the equilibrium excess of population in the absence of the radiofrequency field.

By using Eq. 2.13 for R , we obtain

$$n_s = \frac{N_s}{1 + \frac{1}{2}\gamma^2 H_1^2 T_1 g(\nu)} \quad (3.11a)$$

From Eq. 3.11a we see that when too much radiofrequency power is used, the number of excess nuclei n_s decreases, and so does the resonance signal. We say that the sample has been saturated, and the ratio n_s/N_s is frequently referred to as the saturation factor Z :

$$\frac{n_s}{N_s} = \frac{1}{1 + \frac{1}{2}\gamma^2 H_1^2 T_1 g(\nu)} \equiv Z \quad (3.14)$$

The maximum useful value of the radiofrequency power therefore depends on the relaxation time T_1 . For solids, T_1 is large (it takes a long time

† Let $n = n_{+1/2} - n_{-1/2}$ be the instantaneous excess of nuclei in presence of both radiofrequency and relaxation. The effect of the radiofrequency is to make $n \rightarrow 0$

$$\left(\frac{dn}{dt} \right)_{RF} = -2Rn \quad (3.12)$$

(The factor of 2 arises because each transition up decreases $n_{+1/2}$ by one, and also increases $n_{-1/2}$ by one). The effect of relaxation is to return $n \rightarrow N_s$

$$\frac{d(N_s - n)}{dt} = -(N_s - n) \frac{1}{T_1} = -\left(\frac{dn}{dt} \right)_{\text{relax}} \quad (3.13)$$

Equilibrium is reached when the sum of the two rates in Eqs. 3.12 and 3.13 is zero; that is,

$$-2Rn + \frac{N_s - n}{T_1} = 0$$

which yields Eq. 3.11

$$n = \frac{N_s}{1 + 2RT_1}$$

for the spins to reorient themselves in the equilibrium position), and therefore only weak radiofrequency fields may be applied. For example, for protons in ice $T_1 = 10^4$ sec. On the contrary, in liquids, especially in solutions containing paramagnetic ions, the relaxation time for protons may be as short as $T_1 = 10^{-4}$ sec.

Finally, a concept often used is the spin temperature T_s ; it corresponds to the value of T in the Boltzmann distribution (Eqs. 3.7 and 3.7a) which would produce an excess of nuclei n_s

$$n_s = \frac{N}{2} \frac{\hbar\omega_0}{kT_s} \quad \text{or} \quad T_s = \frac{TN_s}{n_s} = \frac{T}{Z} \quad (3.15)$$

Thus when the spins are saturated, their "temperature" (T_s) becomes very large.

3.2 LINE WIDTH AND THE SPIN-SPIN INTERACTION

Section 3.1 dealt with the interaction of the nuclear spins with the lattice and the way in which this gives rise to a relaxation process which is essential for the observation of energy absorption. It is also possible for a nuclear spin to interact with its neighboring nuclear spins, but without changing the total energy of the spin system.

The effect of the spin-spin interaction, however, is to slightly shift the exact position of the energy level of any individual spin in the external magnetic field. This energy shift does clearly depend on the relative orientation and distance of the spins, and thus is different for each spin, resulting in an apparent broadening[†] of the energy level. Another way of thinking of the spin-spin interaction is that one nuclear spin produces a local magnetic field H_{local} at the position of another spin, which then finds itself in a field

$$H'_0 = H_0 + H_{\text{local}}$$

and consequently has a resonance frequency $\omega'_0 = \gamma H'_0$ slightly different from ω_0 . To estimate this effect, we calculate the magnetic field produced by a magnetic dipole one nuclear magneton strong, at a typical distance of 1 Å. We use the MKS system.

$$H_{\text{local}} \approx \left(\frac{\mu_0}{4\pi} \right) \frac{\mu_N}{r^3} = \left(\frac{\mu_0}{4\pi} \right) \times \frac{e\hbar}{2M_p} \times \frac{1}{r^3}$$

here μ_N is the nuclear magneton and $\mu_0 = 4\pi \times 10^{-7}$ henry/meter is the permeability of free space[‡] and $e\hbar/2M_p$ is the nuclear magneton.

[†] In the classical analogy, we think of the spin-spin interaction as destroying the phase coherence between the precessing spins and the rotating radiofrequency field.

[‡] Not the Bohr magneton.

Thus

$$\begin{aligned} H_{\text{local}} &\approx 10^{-7} \frac{1.6 \times 10^{-19}}{10^{-30}} \times \frac{1}{2} \times \frac{6.582 \times 10^{-22} \text{ MeV-sec}}{(938 \text{ MeV})/c^2} \\ &= 5.6 \times 10^{-21} \times (3 \times 10^8)^2 = 5 \times 10^{-4} \text{ webers/m}^2 = 5 \text{ gauss} \end{aligned} \quad (3.16)$$

which is a significant broadening of the line, even in a field of 10 kilogauss. In liquids and gases, however, the reorientation of the molecules is so fast that the average local field is very close to zero, and therefore very narrow lines can be obtained.

We have already described the width of the resonance line by the function $g(\nu)$ (Eq. 2.12), and we now see that this width is mainly due to the spin-spin interaction. Since $g(\nu)$ has dimensions of $(\nu)^{-1}$, namely, of time, we define one half of its maximum value by T_2

$$\frac{1}{2}g(\nu_0) = T_2 \quad (3.17)$$

where ν_0 is the resonance frequency in the absence of any broadening effects; T_2 is called the *transverse relaxation time*. In view of the normalization condition, Eq. 2.12,

$$\int g(\nu) d\nu = 1$$

which also fixes the dimensions of $g(\nu)$, we see that for broad lines T_2 is short, and for narrow lines, T_2 is long.

With the help of the definition in Eq. 3.17, we can then rewrite for the saturation factor Z (Eq. 3.14) *at resonance*

$$Z_0 = Z(\nu_0) = \frac{1}{[1 + \gamma^2 H_1^2 T_1 T_2]} \quad (3.14a)$$

The width of the resonance line may occasionally also be influenced by very short spin-lattice relaxation, since this limits the "lifetime" of the spins in the upper state; it then follows from the uncertainty principle that the energy level would have a width ΔE . To obtain a width of 5 gauss ($\Delta\nu = \gamma\Delta H/(2\pi)$, which for protons corresponds to 20 kc), T_1 must be†

$$\Delta E \Delta t \sim \hbar \quad T_1 \sim \frac{1}{2\pi(\Delta E/\hbar)} = \frac{1}{6.28 \times 20 \times 10^3} \sim 10^{-5} \text{ sec}$$

Finally, in the experimental observations, spurious broadening effects mainly due to inhomogeneities in the magnetic field must be eliminated first. Clearly, such effects broaden the signal but also decrease its amplitude.

† The same argument also holds for T_2 .

3.3 THE RADIOFREQUENCY MAGNETIC SUSCEPTIBILITIES†

As is known from electrostatics and magnetostatics, when an electric (or magnetic) field E , (or H) is applied in a region containing matter, the material becomes polarized (or magnetized). We write

$$\mathbf{P} = \chi_e \mathbf{E} \quad \mathbf{M} = \chi_\mu \mathbf{H} \quad (3.18)$$

where χ_e and χ_μ are the electric and magnetic susceptibilities and measure the strength of this effect. We now know from the microscopic behavior of matter (atomic and molecular physics) that the polarization is due primarily to the alignment of the electric (magnetic) dipole moments of the atoms or molecules in the direction of the applied field. Materials which have such dipole moments and exhibit large polarization should be called *paraelectric* (or for large magnetization, they are indeed called *paramagnetic*).

Now we also know that the refractive index of light (that is, of a high-frequency electromagnetic field) is related to the electric and magnetic susceptibilities, since

$$\epsilon = (1 + \chi_e) \epsilon_0 \quad \mu = (1 + \chi_\mu) \mu_0$$

and

$$n = \frac{c}{v} = \frac{1/(\sqrt{\epsilon_0 \mu_0})}{1/(\sqrt{\epsilon \mu})} = \sqrt{(1 + \chi_e)(1 + \chi_\mu)}$$

Further, the refractive index (and therefore also the susceptibilities) is a function of the frequency, as we know from the familiar phenomenon of the dispersion of light. Thus we have a susceptibility at optical frequencies which differs from the static one and is a function of the frequency‡. As a matter of fact frequently the transmission of the electromagnetic (light) pulse is accompanied by absorption (which may be strongest at a particular resonant frequency of the atomic oscillators); we may account for the absorption by attributing an imaginary part to the susceptibility.

The same formalism can be used for the description of the nuclear magnetic resonance phenomena as well. The static susceptibility arising from the *nuclear* moments in an otherwise diamagnetic material exists, but is very small and difficult to measure. For the radiofrequency susceptibility, we write

$$\chi(\omega) = \chi'(\omega) - i\chi''(\omega)$$

† This section may be omitted without a loss of continuity and the reader can proceed directly to the discussion of the experimental technique and results in Section 4. However, the discussion should be quite helpful for understanding the meaning of the "dispersion" curve as well as the observed line shapes for both absorption and dispersion.

‡ For optical frequencies and for almost all materials, χ_μ is 0 and the variation in n arises entirely from χ_e .

where both $\chi'(\omega)$ and $\chi''(\omega)$ exhibit a resonant behavior when ω reaches $\omega_0 = \gamma H_0$. The real part $\chi'(\omega)$ is given by

$$\chi'(\omega) = \frac{1}{2} \chi_0 \omega_0 T_2 \left[\frac{(\omega_0 - \omega) T_2}{1 + (\omega_0 - \omega)^2 T_2^2 + \gamma^2 H_1^2 T_1 T_2} \right] \quad (3.19)$$

while the imaginary part $\chi''(\omega)$ is given by

$$\chi''(\omega) = \frac{1}{2} \chi_0 \omega_0 T_2 \left[\frac{1}{1 + (\omega_0 - \omega)^2 T_2^2 + \gamma^2 H_1^2 T_1 T_2} \right] \quad (3.20)$$

Here χ_0 is the static susceptibility defined as in Eq. 3.18

$$M_0 = \chi_0 H_0$$

and T_1 and T_2 are the familiar relaxation times introduced before; the term $\gamma^2 H_1^2 T_1 T_2$ appearing in the denominator is a measure of the saturation as defined in Eq. 3.14.

Equations 3.19 and 3.20 are shown in Fig. 8.5 under the assumption that $\gamma^2 H_1^2 T_1 T_2 \ll 1$; they have the typical behavior of a dispersion and a power resonance curve. We also note that Eq. 3.19 is the derivative, with respect to ω , of Eq. 3.20; by properly adjusting the detection equipment, we may observe experimentally either of those curves (or a combination of both).

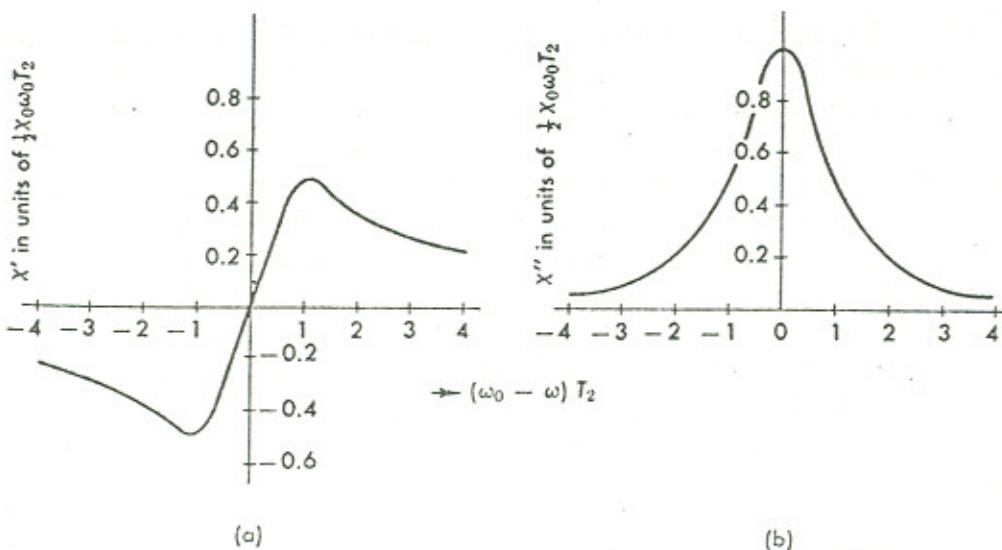


FIG. 8.5 The radiofrequency magnetic susceptibilities near resonance. (a) The real part of the susceptibility exhibits a typical dispersion shape (Eq. 3.19 of text). (b) The imaginary part of the susceptibility exhibits a typical absorption shape (Eq. 3.20 of text).

4. Experimental Observation of the Nuclear Magnetic Resonance of Protons

4.1 GENERAL CONSIDERATIONS

To observe nuclear magnetic resonance we clearly will need a sample, a magnet, a source of electromagnetic radiation of the appropriate frequency, and a detection system.

The magnetic field should be quite homogeneous, and therefore it is advisable to choose a good magnet with polefaces at least 4 to 6 in. in diameter. As discussed in Section 3.2, inhomogeneities in the magnetic field broaden the line (and thus, decrease correspondingly the peak amplitude); to obtain reasonable results, the inhomogeneities over the volume of the sample should be less than 1/1000. The choice of the field strength is arbitrary, provided the resulting frequency lies in a convenient radio-frequency band. However, since the signal-to-noise ratio increases (improves) as $\nu_0^{3/2}$, high fields are preferable; commonly magnets of 5000 to 10,000 gauss strength are used, and for protons this corresponds to frequencies of 20 to 40 Mc/sec.

The sample can be any material containing an ample supply of protons: paraffin, water, mineral oil, or any organic substance containing hydrogens will, in general, give a proton nuclear magnetic resonance signal. Some care must be exercised to avoid materials with long spin-lattice relaxation time T_1 , since they will saturate at very low levels of radiofrequency power (as explained in Section 3.1) and therefore give weak signals. Similarly it is profitable to have a narrow line, hence materials with long spin-spin relaxation time T_2 are chosen. Liquids will meet this condition, and in most instances the width of the line will be determined by the magnet inhomogeneity ($T_2 = 2 \times 10^{-3}$ sec will give for protons a line width of 0.1 gauss). Plain tap water makes a good sample, or tap water doped with one percent by weight of manganese nitrate [$Mn(NO_3)_2$].

The size of the sample is limited again by the area over which the magnet is homogeneous, but also by practical considerations on the coil which is used to couple the radiofrequency to the sample. In usual practice a 1-cm³ sample is adequate; it is contained in a small tubular glass (or other) container, around which is wrapped a radiofrequency coil as shown in Fig. 8.6. The whole assembly is then inserted into the magnet gap and should be secured firmly, since vibration is picked up by the coil and appears as noise in the detectors.

In deriving the probability for a transition between the m sublevels, and in all our previous discussion, we have assumed the existence of a *rotating* field at the angular frequency ω close to ω_0 . In practice, however, a field oscillating linearly, rather than rotating, is established; such a

magnetic field will certainly exist in the interior of the radiofrequency coil shown in Fig. 8.6, and will alternate in direction with a sinusoidal amplitude:

$$A \sin \omega t$$

It is well known, however, that linear harmonic motion is equivalent to two rotations in opposite direction and of amplitude $A/2$ as shown in Fig. 8.7; indeed

$$A \cos \omega t n_x = \frac{A}{2} (\cos \omega t \mathbf{n}_x + (\sin \omega t) \mathbf{n}_y) + \frac{A}{2} (\cos (-\omega t) \mathbf{n}_x + \sin (-\omega t) \mathbf{n}_y) \quad (4.1)$$

where \mathbf{n}_x and \mathbf{n}_y are the unit vectors in the x and y directions. The component rotating in the same direction as the precessing spins will be in resonance and may cause transitions; the other component is completely out of phase and has no effect on the sample.

When the radiofrequency reaches the resonance value ω_0 , energy is absorbed from the field of the coil and this fact is sensed by the detector. Because, however, of the low signal levels involved and the difficulty of maintaining a very stable level of radiofrequency power it is advantageous to traverse the whole resonance curve in a relatively short time. This can be achieved either by "sweeping" the frequency of the radiofrequency oscillator while maintaining the magnetic field constant, or by "sweeping" the magnetic field while the frequency remains fixed. The latter condition

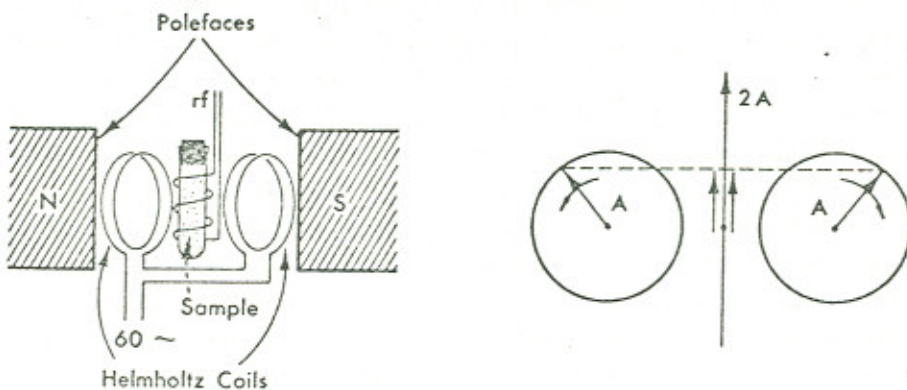


FIG. 8.6 Schematic arrangement of a nuclear magnetic resonance apparatus. The sample is placed in a homogeneous magnetic field and radio frequency is coupled to it by means of the coil. The Helmholtz coils are used to modulate the constant magnetic field.

FIG. 8.7 A linearly oscillating field of frequency ω is equivalent to two fields rotating in opposite directions with the same frequency ω .

can be achieved very easily and is therefore widely used. A small pair of Helmholtz coils[†] is placed across the sample as shown in Fig. 8.6; remember that the constant field H_0 , (and thus also the "sweeping field") must be perpendicular to the radiofrequency field H_1 , which is determined by the axis of the radiofrequency coil. The sweep coils are fed with a slowly varying current[‡], which therefore results in a modulation of the magnetic field H_0 . If this sweep covers the value of H_0 which is in resonance with the fixed frequency of the oscillator, a resonance signal modulated at the frequency of the sweep will appear at the detector. The existence of a modulated signal has the advantage of easier amplification and also presents the possibility of using a narrow band-width detector with the corresponding improvement in the signal-to-noise ratio.

The radiofrequency oscillator and detection circuit can be of several types. In the following sections we describe first a system using a radiofrequency bridge for the detection of resonance; in principle this is the most sensitive technique and can be used for point-by-point measurement of a nuclear magnetic resonance line. Next is presented the marginal oscillator system, which is much more compact and is widely used in commercial nuclear magnetic resonance magnetometers; it gives strong signals for protons but cannot be used for detailed studies of line shapes. Finally, a very simple transistor circuit which yields adequate signals for protons is described.

A different experimental technique for the observation of nuclear magnetic resonance consists in the use of two radiofrequency coils placed 90 degrees with respect to one another, but both lying in the plane normal to H_0 . The radiofrequency is supplied in one coil and the second coil acts as a pickup of the radiofrequency voltage induced by the precessing spins. When the radiofrequency is off resonance, the relative phase of the spins is random and no net induction occurs; when, however, resonance is established, all the precessing spins are brought into phase by the action of the H_1 field and an induction signal appears in the other coil. This method is the one used by Bloch and collaborators, whereas the previously described one-coil method was used by Purcell and collaborators. The experiments discussed below were performed with the one-coil method.

Even though nuclear magnetic resonance studies do provide information on relaxation times and mechanisms, we will restrict the discussion of the results obtained in this laboratory to the observation of the resonance conditions for protons.

[†] A pair of coils of diameter d , spaced a distance $d/2$ apart and traversed by current in the same direction, produce a very homogeneous field at the geometrical center of the configuration.

[‡] Frequently the 60 cps of the a-c line is used; a transformer and variac are placed in the line for reducing and controlling the voltage applied to the coils. See Fig. 8.9.

4.2 DETECTION OF NUCLEAR MAGNETIC RESONANCE WITH A BRIDGE CIRCUIT

It has been noted that a rotating radiofrequency field can be established in the interior of a small coil, where the sample is placed. We wish now to examine how the small absorption of power from the field (Eq. 3.8) may be detected experimentally: we can think of the absorption as a change in the Q value of the coil when the resonant frequency is reached. The Q value, or quality factor, of a device is defined as 2π times the ratio of the time-averaged energy stored to energy dissipated, in one cycle. For a coil of inductance L and resistance R ,

$$Q = \frac{2\pi\omega L}{R} \quad (4.2)$$

When resonance is reached, the magnetic susceptibility (real part, Eq. 3.19) changes, and thus also the inductance of the coil changes. Alternatively, the absorption of power from the field (imaginary part of the susceptibility Eq. 3.20) corresponds to increased dissipation and therefore increased resistivity of the coil. This small change in the Q value (Eq. 4.2) will result in a change of the voltage across the coil if it is driven by a constant current source (as is the case with the transistor circuit of Section 4.4); if a fixed voltage is applied to the coil, the change in Q is best detected with a bridge circuit.

Such a bridge is shown diagrammatically in Fig. 8.8a. The radiofrequency voltage is applied between points a and g , and therefore radiofrequency current flows through the load L and the dummy branch D ; if the bridge

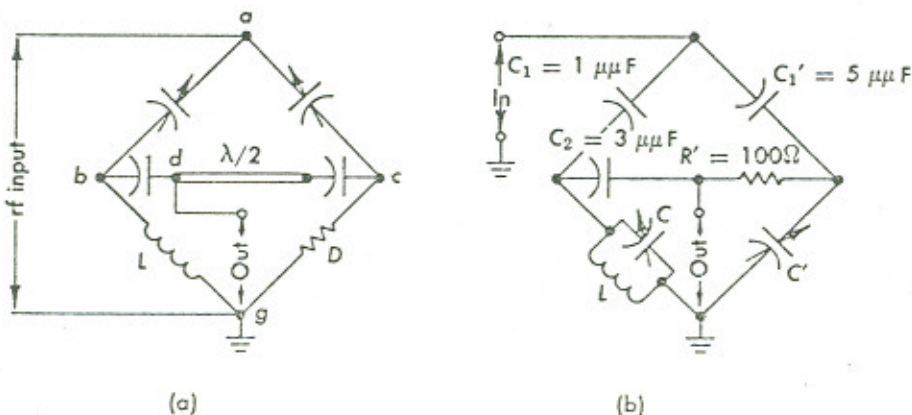


Fig. 8.8 A radiofrequency bridge circuit that can be used for the detection of nuclear magnetic resonance. (a) Schematic arrangement; note that L is the load (radiofrequency coil). The $\lambda/2$ line ascertains cancellation at the output of the signals from b and c . (b) A practical radiofrequency bridge circuit. For resonance conditions see Eq. 4.3 in the text.

is balanced, no voltage should appear at the point d (since b and c were in phase and of the same amplitude, and the signal from c to d is shifted by $\lambda/2$). Any slight unbalance of the bridge produces a small voltage at d . In actual practice, the bridge circuit shown in Fig. 8.8b was used where the $R'C'$ elements are effectively generating the $\lambda/2$ phase shift and L is the sample coil. The conditions for balance† are

$$\text{Resistive balance: } \omega^2 C_1 C_2 \left(1 + \frac{C'}{C'_1} \right) R' R_p = 1 \quad (4.3)$$

$$\text{Reactive balance: } C + C_1 + C_2 \left(1 + \frac{C_1}{C'_1} \right) = \frac{1}{L\omega^2}$$

where R_p is the parallel resistance of the coil. The block diagram of the experimental setup is shown in Fig. 8.9 and consists of the following parts:

- (a) The radiofrequency generator, which in this case was the variable frequency oscillator shown in Fig. 8.10. A crystal-controlled oscillator may be used, especially if only a fixed frequency is to be employed.
- (b) The standard 93-ohm attenuator, which is very convenient in adjusting the power input into the bridge.

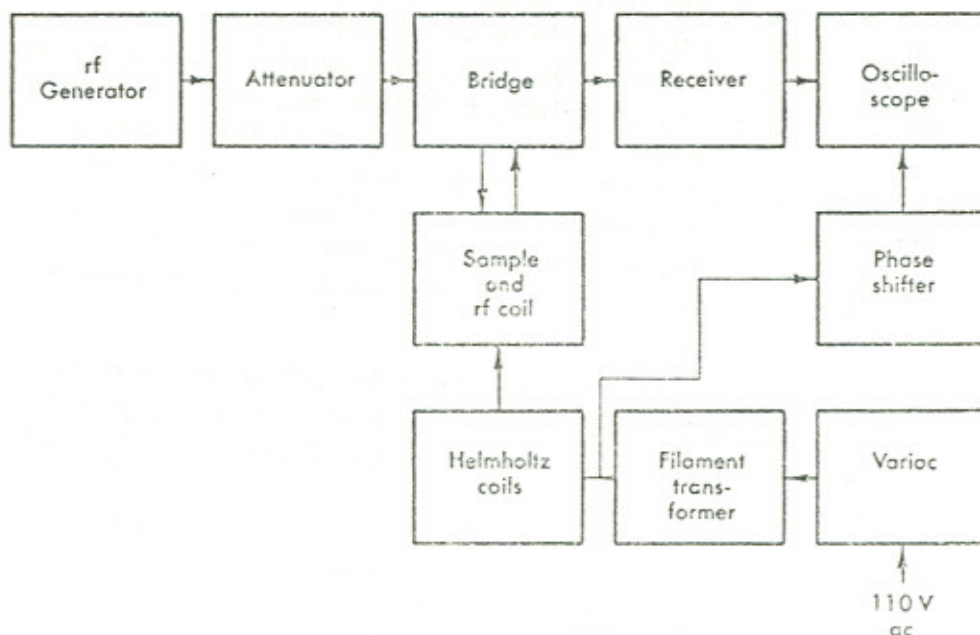


FIG. 8.9 Block diagram of the nuclear resonance measuring apparatus.

† See E. R. Andrew, *Nuclear Magnetic Resonance*, Cambridge University Press, p. 47 and references therein.

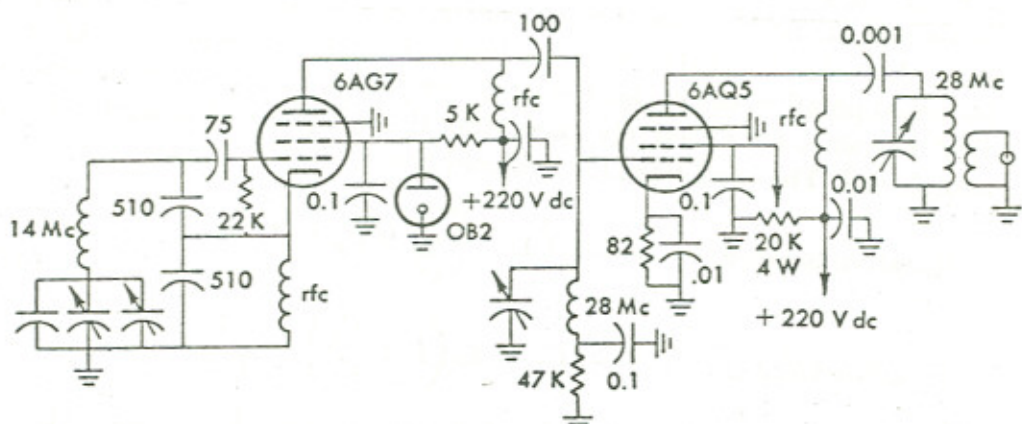


FIG. 8.10 A variable frequency oscillator suitable for providing the radiofrequency for a nuclear magnetic resonance experiment. The frequency is in the range of 28 Mc/sec.

- (c) The bridge (Fig. 8.8b)
- (d) The radiofrequency coil, which is part of the bridge circuit and consists of 6 turns of number 24 wire wound on a glass tube 8 mm in diameter. Its axis clearly must be perpendicular to the constant field H_0 .
- (e) The amplifier. For that purpose a National N.C. 400 radio receiver was used and it was tuned to the frequency of the radiofrequency. The bridge output was fed directly to the N.C. 400 input; the audio stages of the receiver were bypassed and an output signal was taken directly after the second detector stage (First I.F. 1721 kc/sec; second I.F. 445 kc/sec).
- (f) The oscilloscope used for the display of the resonance. The demodulated signal is fed to the vertical input of the oscilloscope, the horizontal sweep being driven by the sweep voltage.
- (g) A phase-shifting network (such as that shown in Fig. 8.11), which is used to allow the positioning of the resonance dip in the center of the oscilloscope sweep.

Frequently, when the voltage for the Helmholtz coils is taken from the line, the oscilloscope may be used with its own linear sweep (1–2 msec/cm on the scope screen is obviously a convenient rate) and triggered from the line voltage.

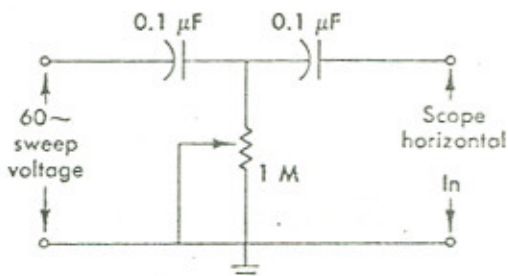


FIG. 8.11 A simple phase-shifting network that can be used to adjust the position of the resonance signal on the oscilloscope trace.

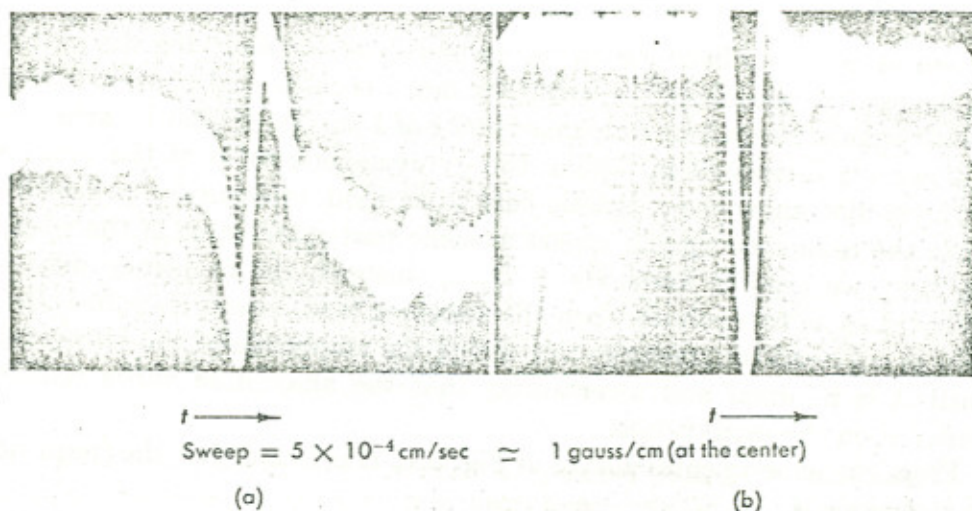


FIG. 8.12 Results obtained from the nuclear magnetic resonance of protons using a bridge circuit. (a) Dispersion curve. (b) Absorption curve. The oscilloscope sweep was linear at 0.5 msec/cm which corresponds to approximately 1 gauss/cm at the center of the sweep.

The bridge is balanced either in the resistive mode, when the change in the Q of the coil will appear as an absorption curve (Fig. 8.5b); indeed, this is observed experimentally, Fig. 8.12b; or the bridge may be balanced in the reactive mode, when the signal appears as a dispersion curve (Fig. 8.5a) and is so observed experimentally, Fig. 8.12a.

The main problem in obtaining a good null for the bridge is to limit the stray radiofrequency power by appropriate shielding; also the mechanical rigidity of the bridge is important. It is advisable to bypass to ground the Helmholtz coils with a small condenser since they pick up radiofrequency.

The experimental results obtained with this arrangement by a student† are shown in Fig. 8.12. The sample was 1 cm³ of water doped with manganese nitrate [$Mn(NO_3)_2$] and the extent of the sweep was approximately 6.2 gauss at 60 cps. The horizontal sweep in the figure is 0.5 msec/cm; Fig. 8.12a shows the dispersion curve whereas Fig. 8.12b shows the absorption curve. Since the oscilloscope sweep is linear at 0.5 msec/cm, the corresponding field change is not linear but of the order of 1 gauss/cm at the center of the sweep (see Section 5.3 also).

To measure the resonance frequency exactly, a precise (crystal controlled) frequency meter is required. The BC 221‡ is convenient, and its variable oscillator is adjusted for zero beat against the radiofrequency

† T. Walters, class of 1962 with the assistance of F. Reynolds.

‡ U. S. Army Signal Corps, BC 221 frequency meter; this may be purchased as army surplus equipment.

generator either by listening on the earphones or by observing the pattern on the oscilloscope. Since the frequency meter is calibrated at each "checkpoint" against its own crystal, an accuracy of 1 part in 10^5 can be achieved.

If we are interested in finding the gyromagnetic ratio of the protons, we must also know the magnetic field to as good an accuracy as possible. Since the resonance signals appear at some particular value of the sweeping field, we need to know $H_0 + H_{\text{sweep}}$; instead, the frequency may be adjusted so as to resonate when the sweeping field crosses its zero value.[†] This is achieved by gradually decreasing the amplitude of the sweep field until it is minimal and ascertaining that the absorption curve remains centered on the oscilloscope.

From the experimental curves of Fig. 8.12 it is found that the frequency at resonance is

$$\nu_0 = 28,141.48 \pm 0.63 \text{ kc/sec}$$

The magnetic field, unfortunately, cannot be measured to similar accuracy; by using a rotating coil flux meter at the field position previously occupied by the sample, it was obtained

$$H_0 = 6642 \pm 20 \text{ gauss}$$

and hence

$$\gamma = (26.618 \pm 0.08) \times 10^3 \text{ rad/sec-gauss}$$

In good agreement with the accepted value

$$\gamma = 26.73 \times 10^3 \text{ rad/sec-gauss} \quad (4.4)$$

The reader will appreciate at this point that it is much easier to measure ratios of nuclear moments to high accuracy than to obtain their absolute value to the same accuracy.

If it is desired to obtain the g factor of the proton—that is, the connection between magnetic moment and the nuclear magneton—we have

$$\mu = gI\mu_N$$

and from Eq. 1.1 and Eq. 2.3

$$\omega_0\hbar = 2\mu H_0$$

$$g = \frac{\omega_0\hbar}{H_0} \frac{1}{2I} \frac{1}{\mu_N} = \frac{1}{2\pi} \frac{\omega_0}{H_0} \frac{1}{2I} \frac{\hbar}{\mu_N} = \frac{1}{2\pi} \gamma \frac{1}{762} \frac{1}{2I} \quad (4.5)$$

[†] Alternatively, the frequency is adjusted so as to resonate at the upper limit of the sweep and it is measured there; next the frequency is adjusted for the lower limit of the sweep and measured again. The difference of the two frequency measurements corresponds to the width of the sweep field (in kilocycles). The central frequency (that is, the frequency corresponding to H_0) is the average value of the two limits.

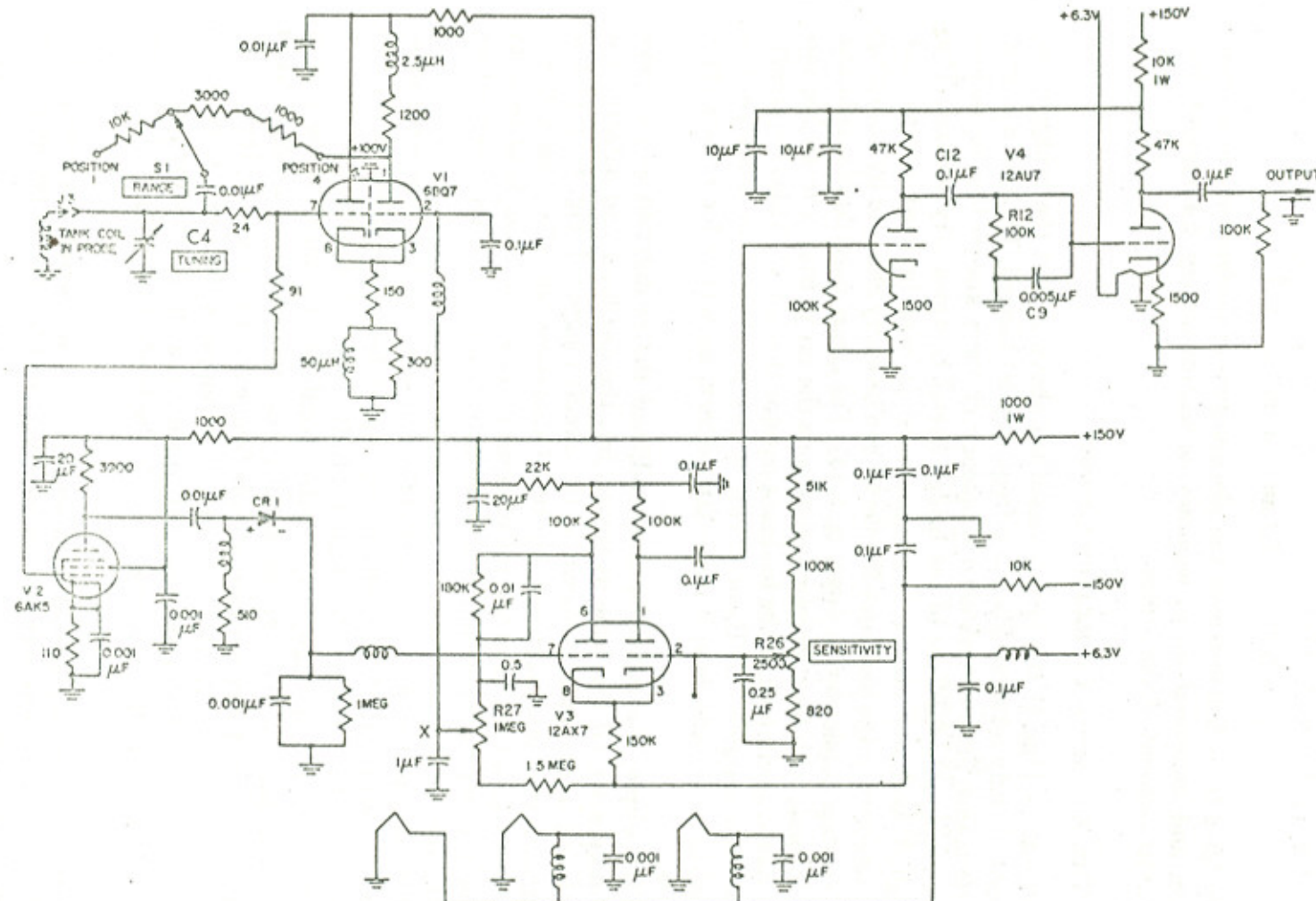


Fig. 8.13 The marginal oscillator circuit; the detection of nuclear magnetic resonance.

using Eq. 1.2 for μ_N/h . Thus

$$g = 5.56 \pm 0.02 \text{ nuclear magnetons}^{\dagger}$$

We have thus demonstrated the phenomenon of nuclear magnetic resonance, and measured to an accuracy of approximately 0.4 percent the magnetic moment of the proton.

4.3 THE MARGINAL OSCILLATOR CIRCUIT

A disadvantage of the system described above is that the bridge must be continuously retuned when the frequency is changed. Thus, in a search for resonance lines of unknown frequency or for a known line in an unknown magnetic field use of the bridge circuit becomes very tedious. The marginal oscillator circuit is compact and is used in most commercial magnetometers; the oscillator frequency can be easily changed by adjusting the variable condenser C_4 (see Fig. 8.13). For larger variations a different coil is used; with four radiofrequency coils the range from 1 to 40 Mc can be covered (switching of the feedback resistor through S_1 is also required). While the marginal oscillator circuit is less sensitive than a bridge, the signal-to-noise ratio is still quite satisfactory, especially for proton resonance.

The sample, the radiofrequency coil, and the modulation and display techniques are all the same as before, but the oscillator and detector are combined in one unit as shown in the circuit diagram,‡ Fig. 8.13, of the magnetometer manufactured by the Laboratory for Electronics Corp. The main idea is to keep the radiofrequency power at a low level so as to allow the direct observation of the absorption and also to avoid saturation of the sample.

Referring to Fig. 8.13, we see that the two sections of V_1 form a cathode-coupled oscillator, the radiofrequency signal being amplified in V_2 and rectified in CR_1 . The rectified signal is further amplified in the two sections of V_3 . However, through R_{27} , negative feedback is applied to the grid of V_{1B} ; this has the effect of maintaining the radiofrequency oscillations at a low level since any increase in radiofrequency appears as a drop in the d-c level at point X , which thus tends to suppress the oscillations of V_1 . It is possible with this arrangement to sustain a steady radiofrequency at a level as low as 0.1 V across the coil; the level can be adjusted through R_{26} and R_{27} .

† The fact that the g factor of the proton is not 2.00, as expected for a Dirac particle, tells us that interactions other than electromagnetic are responsible for this large "anomalous" magnetic moment.

‡ Transistorized versions of this circuit are now available; see, for example, the AL 67 nuclear magnetic resonance gaussmeter manufactured by Alpha Scientific Labs Inc.

When resonance is reached, the change in the Q value of the coil results in a small decrease of the radiofrequency level. If the magnetic field is swept at a low frequency, the absorption dip will appear as a small amplitude modulation of the rectified radiofrequency. This audio signal is finally amplified in V_4 whose two sections form a narrow band-width amplifier in order to reduce noise; the amplifier is tuned to 60 cps through the C_{12} , R_{12} , and C_9 network. With this circuit, only the absorption mode is observed; also it is not possible to investigate a line "point by point."

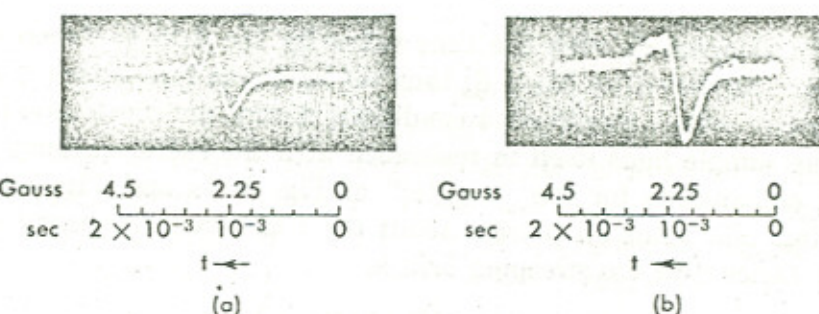


FIG. 8.14 Nuclear magnetic resonance signals of protons obtained with the marginal oscillator circuit. (a) The sample is water doped with manganese nitrate; note the "wiggles" after passage through resonance. (b) The sample is mineral oil.

In Fig. 8.14 are shown oscilloscope traces obtained by students using the marginal oscillator as described above;[†] Fig. 8.14a is obtained with the same sample previously mentioned, water doped with $Mn(NO_3)_2$, and Fig. 8.14b with a sample of mineral oil; for both cases resonance occurs at the same frequency $\nu = 28.189 \pm 0.003$ Mc/sec. The sweeping field was a 60 cps sine wave with maximum amplitude of 6 gauss, and thus a sweeping rate[‡] of

$$\frac{dH}{dt} \approx 2.25 \times 10^3 \text{ gauss/sec} \quad (4.6)$$

The oscilloscope sweep was linear and set to 0.2 msec/cm, so that the horizontal scale calibration is ~ 0.45 gauss/cm.

We note that Fig. 8.14b looks almost like the predicted absorption line of Fig. 8.5b (inverted), but Fig. 8.14a has a distinctly different shape and is followed, *after* passage through resonance, by decaying oscillations. In both cases the deviation from the theoretical line shape is due to the fast

[†] M. Klein and P. D'Onofrio, class of 1962.

[‡] If at $t = 0$ the amplitude of the sweep field is to have its central value, which is 0, then $H_{\text{sweep}} = H_s \sin \omega t$ and $dH/dt = \omega H_s \cos \omega t$, which is almost linear for $t \approx 0$ and $dH/dt \approx \omega H_s$.

passage through resonance, which gives rise to "transient effects"; by fast is meant fast as compared to the characteristic relaxation times of the system.

Indeed, from Fig. 8.14b we estimate the width of the line to be $\Delta H \approx 0.4$ gauss full width at half maximum (fwhm), and using Eq. 3.17† we obtain

$$T_2 = \frac{1}{2}g(\nu_0) = \frac{1}{2\Delta\nu} = \frac{\pi}{\Delta\omega} = \frac{\pi}{\gamma\Delta H} = \frac{3.14}{2.67 \times 10^4 \times 0.4} \sim 3 \times 10^{-4} \text{ sec}$$

(4.7)

which is comparable with the time taken by the field to sweep over the resonance as shown by Eq. 4.6; thus the spin-spin interaction hardly has the time to restore equilibrium conditions during the short time interval‡ that the sample finds itself in resonance with the radiofrequency.

The explanation for the "wiggles" of Fig. 8.14a and Fig. 8.16 is the following. The spins all precess about the z axis at a frequency ω , which slowly varies with the sweeping field as

$$\omega = \gamma(H_0 + H_{\text{sweep}}) \quad (4.8)$$

However, the spins are not in phase; that is, their azimuthal angle ϕ is random. When the field reaches an H value such that the precession frequency ω equals the applied radiofrequency ω_0 , resonance occurs and all the spins are brought into phase (that is, they all cluster in the azimuthal plane of the rotating radiofrequency field H_1). As the constant field increases beyond the resonance value, the spins continue to precess at the frequency ω , which again differs from ω_0 , but they remain in phase for a time interval of the order of T_2 . However, such coherently precessing spins will induce in the radiofrequency coil a voltage at the frequency ω ; the two close frequencies ω of the precessing spins and the applied ω_0 which are not exactly equal will interfere (beat) as their relative phase angle

† For simplicity we have assumed $g(\nu)$ to have a triangular shape (see Eq. 2.12). Using

$$\int g(\nu) d\nu = 1$$

we have

$$1 = \frac{1}{2}g(\nu_0)(2\Delta\nu).$$

Similarly, for a Gaussian we obtain

$$T_2 = \frac{1}{2}g(\nu_0) = \frac{2}{\gamma\Delta H}$$

‡ The reader may recognize that this is only a case of a generalized uncertainty principle in experimental procedure. With a detector of band width Δf , the signal-to-noise ratio improves with decreasing Δf as $S/N \propto 1/\sqrt{\Delta f}$; however, for a given Δf , we must wait at least a time interval $\Delta t \sim 1/\Delta f$ in order to make even an approximate measurement, and for an accurate value several time constants Δt need to have elapsed.

changes; this results in the "wiggles" we observe. They do decay exponentially as the phase coherence of the precessing spins becomes destroyed with a time constant T_2 .

If a linear sweep is assumed, the beat signal has the form

$$e^{-t/T_2} \cos \left[\frac{1}{2}\gamma \frac{dH}{dt} t^2 \right] \quad (4.9)$$

where $t = 0$ when resonance is traversed. We also note that the beat frequency increases with time since

$$\omega_b = \frac{1}{2}\gamma \frac{dH}{dt} t \quad (4.10)$$

Thus, from a measurement of the wiggle pattern, information about T_2 can be obtained.

When T_2 is long, and sufficient radiofrequency power is applied, it is possible that the phase coherence may not have completely decayed before the magnetic field value H again approaches resonance; in this case wiggles are also observed before resonance as shown in Fig. 8.15a, taken with a linear time sweep of 0.2 msec/cm ; Fig. 8.16 is a semilog plot of the amplitude of the wiggles (after resonance) of Fig. 8.15a against time. We see that the data fit an exponential, and yield

$$T_2 \approx 5 \times 10^{-4} \text{ sec}$$

of the same order as given by Eq. 4.7.

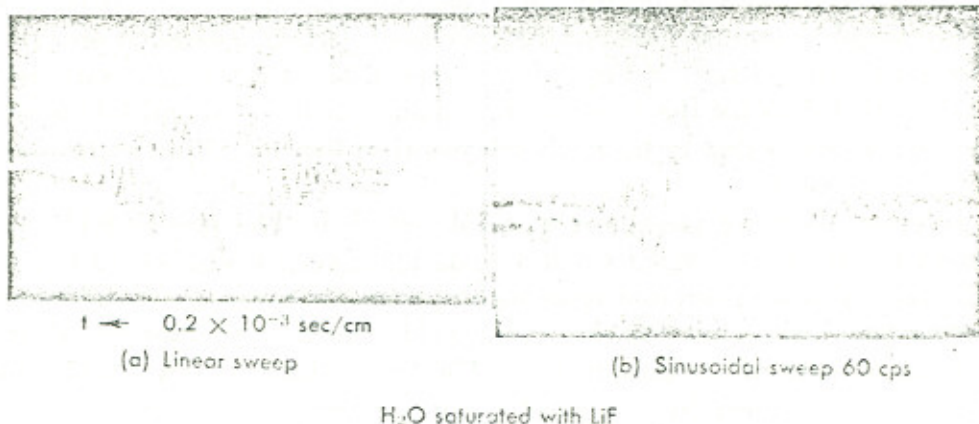


FIG. 8.15 Nuclear magnetic resonance signals for protons when the passage through resonance is very rapid. The sample is water saturated with lithium fluoride. (a) The oscilloscope sweep is linear; note that passage through resonance occurs only once. (b) The oscilloscope sweep is sinusoidal and passage through resonance occurs twice.

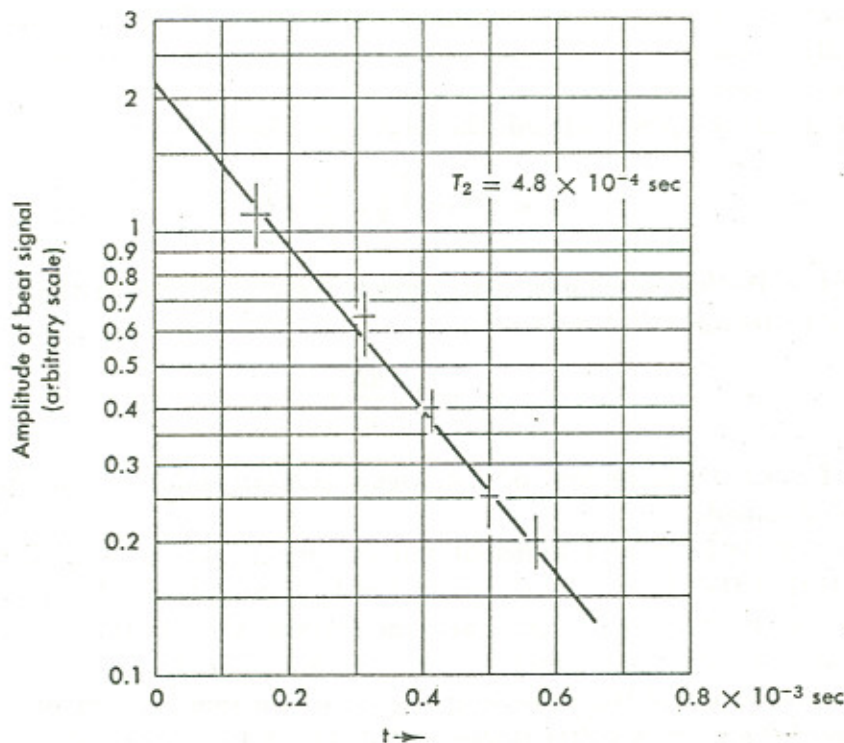


FIG. 8.16 Semilog plot of the amplitude of the "wiggles" of the resonance signal shown in Fig. 8.15 plotted against time. Note that it yields an exponential decay of the amplitude with a characteristic time constant of 4.8×10^{-4} sec.

Just as the inhomogeneity of the magnetic field will broaden the line, however, so it will also destroy the phase coherence (since different parts of the sample precess at different frequencies ω). In fact, a detailed analysis[†] shows that the pattern of Fig. 8.15a is typical of an inhomogeneous field. Thus both values for the effective T_2 obtained in Eqs. 4.8 and 4.12 are to be interpreted as due to field inhomogeneities; the true T_2 time for these samples is longer.

In concluding, we mention Fig. 8.15b, which is the same as 8.15a but shows the resonance signal when a sinusoidal sweep is applied to the oscilloscope x axis. Therefore resonance appears twice on the oscilloscope, during both increasing and decreasing field; also now the horizontal axis is linear in field rather than in time. The traces shown in Figs. 8.15a and 8.15b were obtained by students[‡] using a saturated solution of lithium fluoride (LiF) in water. The sweeping field was at 60 cps and had a maximum value of the order of 10 gauss.

[†] E. R. Andrew, loc. cit., p. 134.

[‡] D. Boyd and P. Nichols, class of 1963.

4.4 TRANSISTORIZED NUCLEAR MAGNETIC RESONANCE DETECTOR

As a final example we present in Fig. 8.17 a simple transistor circuit† which can be used for the observation of proton nuclear magnetic resonance. Transistor T_1 (2N502) is the oscillator, feedback being provided by a $10-\mu\text{F}$ capacitor from the collector to the emitter. The frequency is determined by the LC circuit formed by the radiofrequency (the sample) and the variable condenser; it is possible to vary the frequency continuously from 2 to 80 Mc/sec by using coils of the appropriate inductance for each of four ranges. Diode D_1 (1N56) rectifies the radiofrequency and T_2 (2N247) amplifies the audio signal. The output is fed directly to an oscilloscope. The radiofrequency level is adjusted by varying the 10-K potentiometer in the emitter of T_1 .

As before, the sample is 1 cm^3 of water that is doped with manganese nitrate [$\text{Mn}(\text{NO}_3)_2$] and is placed inside the radiofrequency coil; the field is modulated at 60 cps. The important difference between this and the previous circuit is that transistors are *constant current* sources. Thus out of the collector of T_1 flows a current whose amplitude depends on the base-emitter bias, and the radiofrequency voltage at point A is entirely determined by the impedance of the LC circuit. Any change in the Q of the coil appears immediately as a change in the radiofrequency level at point A (or B). This is the fact that accounts for the great simplicity of the circuit of Fig. 8.17.

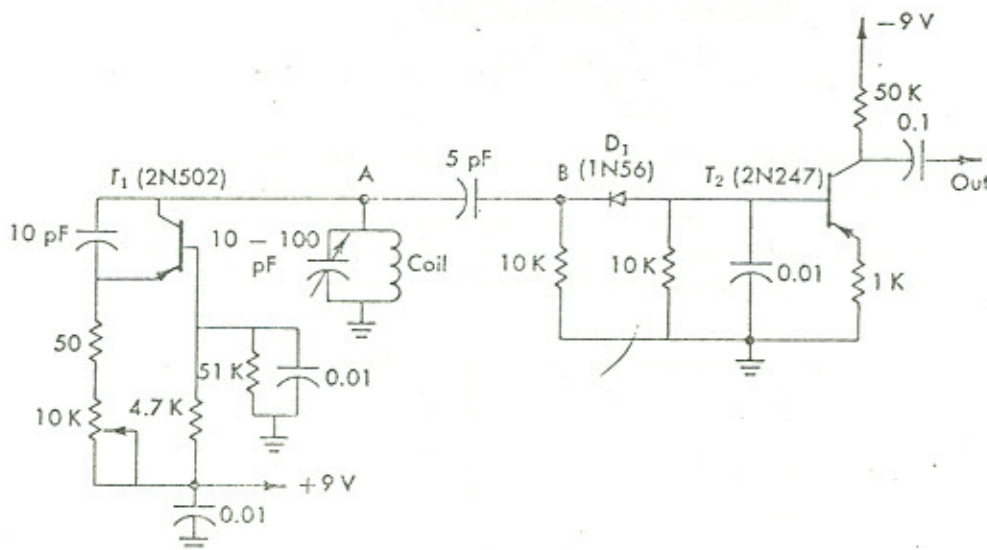


FIG. 8.17 A simple transistorized nuclear magnetic resonance circuit.

† J. R. Singer and S. D. Johnson, *Rev. Sci. Instr.*, 30, 92 (1959).

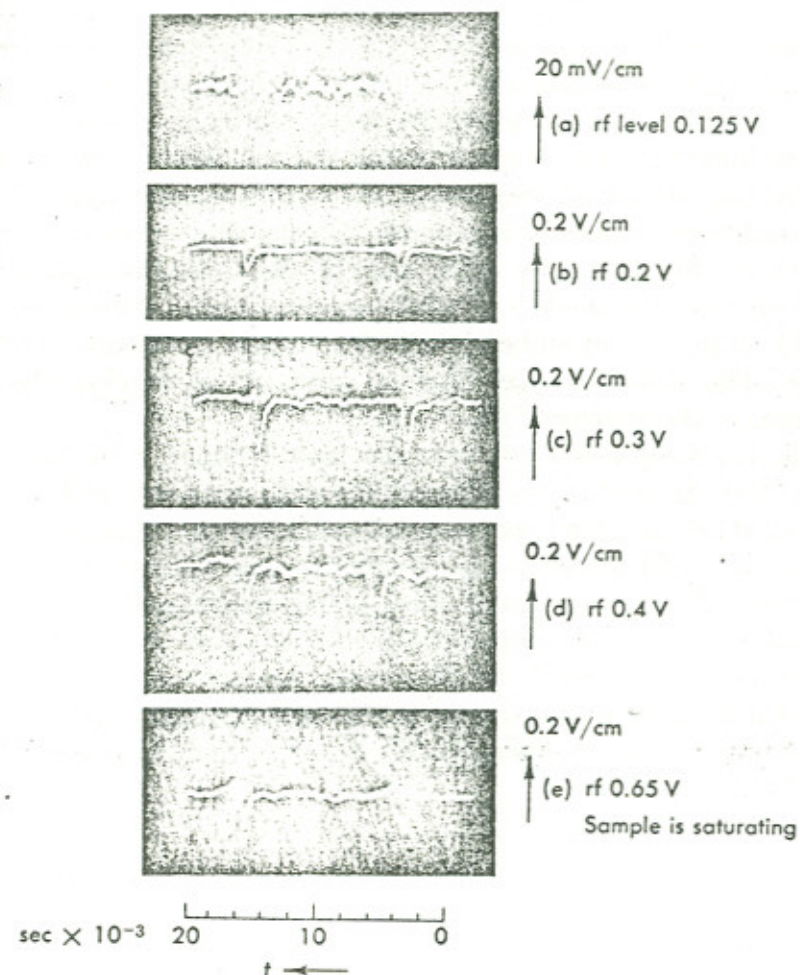


FIG. 8.18 Nuclear magnetic resonance signals from protons obtained with the circuit shown in Fig. 8.17 as a function of the amplitude of the radiofrequency. Note that initially the output signal increases with increasing radiofrequency but at a level of approximately 0.5 V the sample is saturating and the signal begins to decrease.

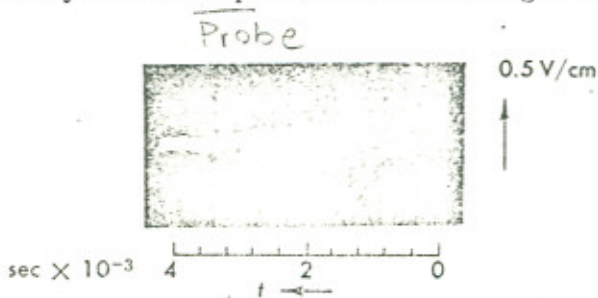


FIG. 8.19 Proton nuclear magnetic resonance signal obtained with the circuit shown in Fig. 8.17 and displayed on an expanded time scale. The magnetic field is of the order of 8 kilogauss.

Data obtained by a student† using this circuit at a frequency of 33,830 Mc/sec are shown in Fig. 8.18 for various levels of radiofrequency voltage across the coil. The magnet was swept at 60 cps, and the oscilloscope sweep is linear at 2×10^{-3} sec/cm; the vertical scale is 200 mV/cm for all but trace (a) where the gain was turned up by a factor of 10. We note that as the level of the radiofrequency is increased, the output at the collector of T_2 increases also; however, for radiofrequency levels beyond ≈ 0.5 V the output level begins to decrease as shown in Fig. 8.18; it almost disappears at ≈ 0.8 V. This is due to the saturation of the sample with increasing H_1 as discussed before and predicted by Eq. 3.14. Finally, in Fig. 8.19 the resonance signal for 0.6 V of radiofrequency and with an expanded horizontal scale of 0.4×10^{-3} sec/cm is shown, indicating clearly the "wiggles" after passage through resonance.

